Regulation and localization of tyrosine^{216} phosphorylation of glycogen synthase kinase-3β in cellular and animal models of neuronal degeneration

Ratan V. Bhat*, Jason Shanley, Maryann P. Correll, William E. Fieles, Richard A. Keith, Clay W. Scott, and Chi-Ming Lee

Neuroscience Department, AstraZeneca Pharmaceuticals, 1800 Concord Pike, Wilmington, DE 19850-5437

Edited by Solomon H. Snyder, Johns Hopkins University School of Medicine, Baltimore, MD, and approved July 19, 2000 (received for review June 28, 2000)

Inactivation of glycogen synthase kinase-3β (GSK3β) by S^9 phosphorylation is implicated in mechanisms of neuronal survival. Phosphorylation of a distinct site, Y^{216}, on GSK3β is necessary for its activity; however, whether this site can be regulated in cells is unknown. Therefore we examined the regulation of Y^{216} phosphorylation on GSK3β in models of neurodegeneration. Nerve growth factor withdrawal from differentiated PC12 cells and staurosporine treatment of SH-SY5Y cells led to increased phosphorylation at Y^{216}, GSK3β activity, and cell death. Lithium and insulin, agents that lead to inhibition of GSK3β and adenoviral-mediated transduction of dominant negative GSK3β constructs, prevented cell death by the proapoptotic stimuli. Inhibitors induced S^9 phosphorylation and inactivation of GSK3β but did not affect Y^{216} phosphorylation, suggesting that S^9 phosphorylation is sufficient to override GSK3β activation by Y^{216} phosphorylation. Under the conditions examined, increased Y^{216} phosphorylation on GSK3β was not an autophosphorylation response. In resting cells, Y^{216} phosphorylation was restricted to GSK3β present at focal adhesion sites. However, after staurosporine, a dramatic alteration in the immunolocalization pattern was observed, and Y^{216}-phosphorylated GSK3β selectively increased within the nucleus. In rats, Y^{216} phosphorylation was increased in degenerating cortical neurons induced by ischemia. Taken together, these results suggest that Y^{216} phosphorylation of GSK3β represents an important mechanism by which cellular insults can lead to neuronal death.

Aberrant cell death within the adult central nervous system is a key mechanism thought to underlie the pathology of several neurodegenerative diseases (1, 2). Survival growth factors protect neurons from a variety of proapoptotic stimuli, and one of the protective mechanisms has been attributed to the activation of the phosphoinositide-3 kinase signal transduction pathway (3). A downstream effector of this signaling pathway is Akt, a kinase that phosphorylates the serine/threonine kinase GSK3β on S^9 to render it inactive (4, 5), a proposed mechanism by which neurons become resistant to apoptotic stimuli (6–8).

A second regulatory site (Y^{216}), which lies within the activation loop between subdomains VII and VIII of the catalytic domain, has been identified on GSK3β and whose phosphorylation is necessary for functional activity (9). Dephosphorylation with a protein tyrosine phosphatase or mutation of Y^{216} on GSK3β results in a dramatic decrease in activity (9). It is unclear whether Y^{216} is a site for GSK3β autophosphorylation or whether a separate tyrosine kinase phosphorylates this site to activate GSK3β (10).

In addition to its role in apoptosis, GSK3β hyperphosphorylates the microtubule-associated protein τ, a mechanism implicated in paired helical filament formation in Alzheimer's disease (11, 12). Despite progress in defining growth factor-dependent pathways that regulate S^9 phosphorylation (13), little is known regarding the regulation of GSK3β activity by Y^{216} phosphorylation in neurons. As a first step, we have determined whether the Y^{216} residue on GSK3β is subject to regulation in models of neurodegeneration. Our results indicate that Y^{216} phosphorylation on GSK3β is robustly increased in response to apoptotic stimuli in neuronal cells and in brain. Y^{216}-phosphorylated GSK3β is localized to focal adhesion points that are disrupted after an apoptotic stimulus and selectively increase within the nucleus. The increased Y^{216} phosphorylation does not occur via an autophosphorylation mechanism, implying that in neurons, proapoptotic stimuli lead to activation of an undetermined tyrosine kinase pathway leading to the phosphorylation of GSK3β on Y^{216} and its activation.

Materials and Methods

Materials. Rat pheochromocytoma (PC12) cells and human neuroblastoma SH-SY5Y cells were obtained from American Type Culture Collection (Rockville, MD). Antibodies and sources: polyclonal phospho-specific Y^{216} and S^9 GSK3β antibodies (QCB-Biosource International, Camarillo, CA); monoclonal GSK3β antibody (Transduction Laboratories, Lexington, KY); monoclonal vinculin antibody, nerve growth factor (NGF) (2.5S), and polyclonal anti-NGF (Sigma); Texas red-labeled phalloidin, Oregon green 488-labeled goat anti-rabbit, and Texas red-labeled goat anti-mouse secondary antibodies (Molecular Probes). Recombinant human (rh) GSK3β was provided by Philip Cohen, University of Dundee, Dundee, Scotland, U.K. The elongation initiation factor 2b peptide substrate was provided by Peninsula Laboratories. γ^{33}P-ATP (specific activity 10 μCi/μl) was from Amersham Pharmacia Biotech.

Apoptosis Induction. PC12 cells were differentiated for 9–12 days in RPMI containing 1% FBS and 50 ng/ml NGF. Apoptosis was induced by washing cells with NGF-free medium and was accelerated by the addition of anti-NGF antibodies (1:400). In SH-SY5Y cells, apoptosis was induced by using staurosporine (0.1–0.3 μM). Quantification of apoptosis was done by measuring fragmented DNA by using a Cell Death Detection kit as specified by the manufacturer (Boehringer–Mannheim, catalogue no. 1774425).

Immunoprecipitation and Kinase Assay. For immunoprecipitation, 10 μg of cell lysate prepared in ice-cold lysis buffer (10 mM

This paper was submitted directly (Track II) to the PNAS office.

Abbreviations: GSK3β, glycogen synthase kinase-3β; NGF, nerve growth factor; MCAO, middle cerebral artery occlusion; rh, recombinant human; HA, hemagglutinin; wt, wild type.

*To whom reprint requests should be addressed at: AstraZeneca R&D Södertälje, B218:318, S-151 85 Södertälje, Sweden. E-mail: Ratan.Bhat@AstraZeneca.com.

The publication costs of this article were defrayed in part by page charge payment. This article must therefore be hereby marked "*advertisement*" in accordance with 18 U.S.C. §1734 solely to indicate this fact.

Article published online before print: *Proc. Natl. Acad. Sci. USA*, 10.1073/pnas.190297597. Article and publication date are at www.pnas.org/cgi/doi/10.1073/pnas.190297597

Tris·HCl, pH 7.5/50 mM NaCl/30 μM $Na_4P_2O_7$/1% Triton-X/0.2 mM PMSF/7.5 μg/ml leupeptin/7 μg/ml each pepstatin A, aprotinin, and E-64/10 μg/ml benzamidine/2 mM Na_3VO_4/2.5 mM NaF) was incubated with 5 μl antibody for 1 h at 4°C followed by overnight incubation with 75 μl of protein G-Sepharose beads. For GSK3β kinase assays, immune complexes were washed with lysis buffer and once with 100 μl kinase buffer [100 mM 4-morpholinepropanesulfonic acid (Mops), pH 7.0/2 mM EDTA]. Kinase assays were performed with either 35 μl immunoprecipitate or 0.4 units/ml of rhGSK3β, 4 μM elongation initiation factor 2b substrate peptide [Ac-RRAAEELDSRAGS(p)PQL]/10 μM γ^{33}P-ATP (0.2 μCi)/10 mM $Mg(Ac)_2$/10 mM Mops, pH7.0/0.2 mM EDTA in a total volume of 50 μl. Reaction was initiated with ATP (30 min at 30°C) and was stopped by spotting 40 μl onto P81 phosphocellulose paper filters. Filters were washed with 75 mM phosphoric acid, rinsed with acetone, and quantitated by scintillation counting. Western blotting and detection were performed as previously described by using antibodies at 1:1,000 dilution (14).

Construction of Vectors for Homologous Recombination in Bacteria. pAdeasy-1, pAdTrack-CMV plasmids and *Escherichia coli* BJ5183 were obtained from Bert Vogelstein, The Johns Hopkins Oncology Center, Baltimore, MD. GSK3β cDNA was obtained from the American Type Culture Collection image clone collection. A hemagglutinin (HA) epitope tag was introduced by PCR, and the construct was cloned into pAd-CMVtrack by using *Bgl*II and *Eco*RV sites. The K85R and Y216F mutations were generated by point mutagenesis of the GSK3β clone by using the QuickChange Kit from Stratagene. Constructs were verified by sequencing and restriction digest.

Recombinant adenoviruses of wild-type (wt) and mutant GSK3β constructs were produced by using the AdEasy System, Quantum Biotechnologies (Montreal, Canada). Cell number was estimated by counting, and the appropriate multiplicity of infection was delivered. Infection was performed in 2% serum (2 h), then normal serum was added for 12 h.

Cerebral Ischemia Model. Long–Evans rats (180–220 g) were given food and water *ad libitum* and housed in an American Association for the Accreditation of Laboratory Animal Care accredited facility. Animals were injected s.c. with lithium chloride or saline, once daily for 16 days (1.5 meq/kg day 1–4; 2.3 meq/kg day 5–11; 3 meq/kg day 12–16), as previously described (15). Twenty-four hours after the last injection, rats were subjected to unilateral cerebral ischemia by 90 min of filament-induced middle cerebral artery occlusion (MCAO), as described (15). The infarcted area (mm^3) for each slice was determined by an image analyzer. For immunohistochemistry, tissue was processed as described previously (14).

Confocal Microscopy and Immunohistochemistry. SH-SY5Y cells grown on coverslips were fixed in 4% paraformaldehyde in PBS at reverse transcription (RT) for 15 min. Cells were permeabilized in 0.2% Triton X-100 in PBS and blocked in 1% BSA in PBS for 15 min. Primary and secondary antibody incubations [rabbit anti-Y ^{216} (1:500) or mouse anti-vinculin (1:500) in blocking reagent, goat anti-rabbit conjugated with Oregon Green 488 (1:1,000)], or goat anti-mouse conjugated with Texas red (1:1,000) or Texas red phalloidin (1:100) were done for 30 min at RT. Each step was followed by a 15-min wash with PBS. Coverslips were mounted in Vectashield (Vector Laboratories) and photographed on an Olympus Fluoview 300 (Olympus, New Hyde Park, NY) confocal microscope by using a ×100 objective.

Results

Apoptotic cell death was measured after NGF deprivation in PC12 cells by using an assay that detects fragmented DNA, a phenomenon associated with endonuclease cleavage of DNA into 180 base pairs during apoptosis. Apoptosis was observed within 3 h after NGF withdrawal and remained elevated for 24 h (Fig. 1*A*). At 3 h after NGF withdrawal, Hoescht staining confirmed that 20–25% of cells exhibited apoptotic morphology. To test whether GSK3β activity was altered in the apoptosis model, we performed a GSK3β kinase assay on proteins immunoprecipitated from cell lysates with a monoclonal GSK3β antibody. NGF withdrawal (3 h) resulted in a 6-fold increase in GSK3β activity that was blocked by lithium (10 mM) or insulin

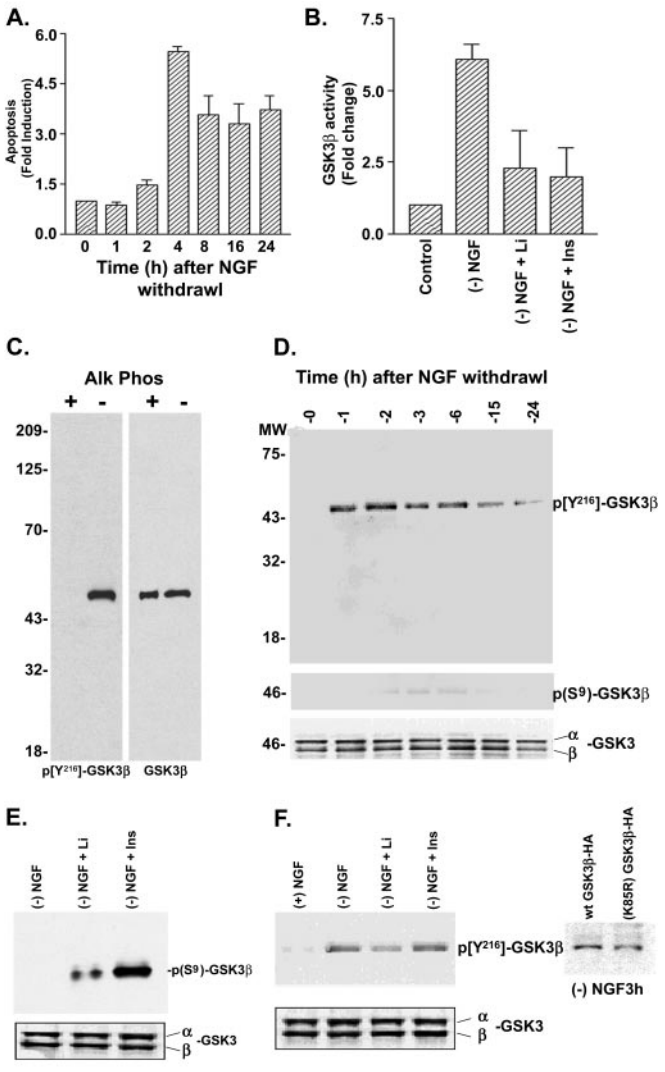

Fig. 1. Regulation of Y^{216} phosphorylation by NGF withdrawal in PC12 cells. (*A*) Quantification of NGF withdrawal induced apoptosis in PC12 cells by using a DNA fragmentation assay (mean ± SEM, $n = 3$). (*B*) GSK3β activity was measured by immunoprecipitation followed by a kinase assay. Cells treated with 10 mM lithium chloride (Li) or 1 μM insulin (Ins) had decreased GSK3β activity. (*C*) (*Left*) Western blot showing that the phospho-Y^{216} specific GSK3β antibody recognizes active rhGSK3β (from Sf9 cells) but not rhGSK3β treated with alkaline phosphatase. (*Right*) Western blot reprobed with an antibody to total GSK3β. (*D*) Blot showing increased Y^{216} phosphorylation after NGF withdrawal (*Top*) but negligible changes at the S^9 phosphorylation site (*Middle*). (*Bottom*) Total levels of GSK3β. (*E*) Western blots showing increased GSK3β phosphorylation on S^9 by lithium and insulin, but no significant reduction in Y^{216} phosphorylation (*F*), assessed at 3 h after NGF withdrawal. (*F Far Right*) Immunoprecipitation by anti-HA antibody and Western blot showing Y^{216} phosphorylation of wt GSK3β-HA and K85R-GSK3β-HA after NGF withdrawal (3 h).

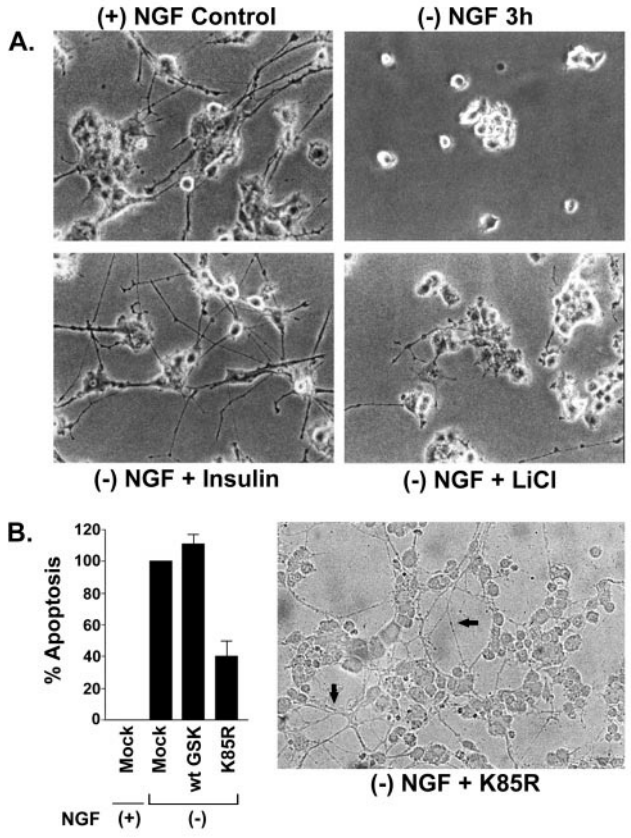

Fig. 2. GSK3β inhibition prevents NGF- withdrawal-induced apoptosis in PC12 cells. (*A*) Photomicrographs of differentiated PC12 cells undergoing apoptosis as a result of NGF withdrawal (*Top Left*). Lithium (10 mM) pretreatment or addition of insulin (1 μM) prevented apoptosis and maintained relative intact cell morphology. (*B*) (*Left*) Effects of adenoviral-mediated transduction of mock (empty vector), wt GSK3β, or dominant negative K85R-GSK3β on apoptosis in PC12 cells. Apoptosis was measured by using the DNA fragmentation assay. K85R-GSK3β protected against NGF withdrawal-induced apoptosis. (*Right*) Photomicrograph of PC12 cells infected with K85R-GSK3β showing intact neurites (arrows) after withdrawal of NGF.

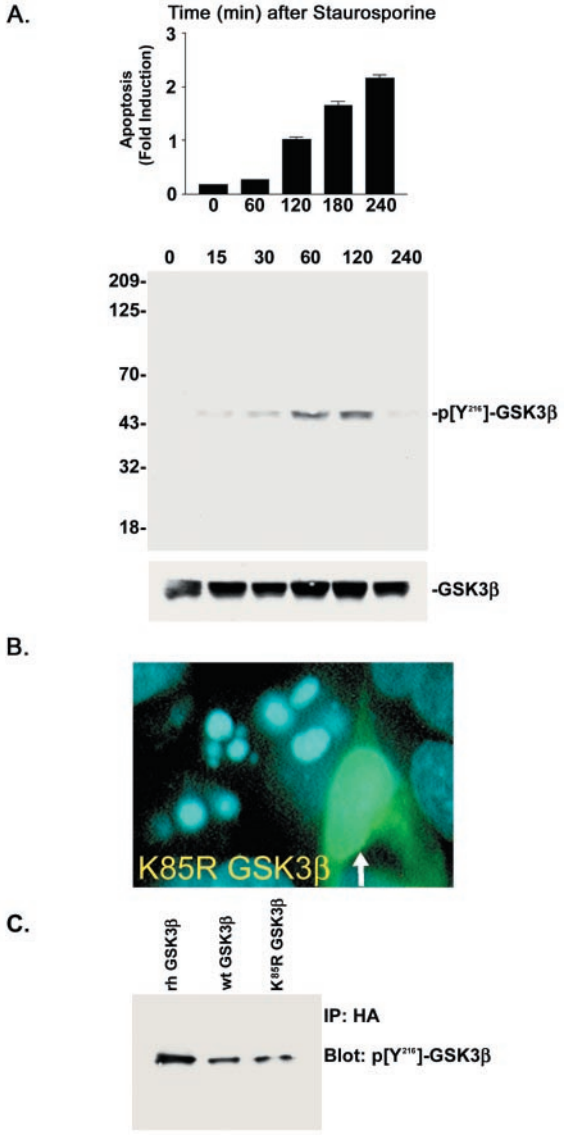

Fig. 3. Regulation of Y^{216} phosphorylation by staurosporine in SH-SY5Y cells. (*A*) (*Top*) Apoptosis was quantified in SH-SY5Y cells treated with staurosporine (0.1 μM) by using the DNA fragmentation assay (mean $\pm$ SEM, $n = 3$). (*Middle*) Western blot showing an increase in Y^{216} phosphorylation after staurosporine treatment. (*Bottom*) Total levels of GSK3β in the samples (*B*). Representative photomicrograph of SH-SY5Y cells infected with dominant negative K85R-GSK3β after 1 h of staurosporine. Infected cell (arrow) exhibited intact nuclear morphology. (*C*) Immunoprecipitation and Western blot examining the Y^{216} phosphorylation of wt GSK3β-HA and K85R-GSK3β-HA expressed in cells treated with staurosporine (1 h). Immunoprecipitation was accomplished by using an HA antibody followed by immunoblotting with the phospho Y^{216} antibody.

(1 μM), treatments known to result in inhibition of GSK3β activity (Fig. 1*B*).

In vitro studies indicate that phosphorylation of Y^{216} residue on GSK3β is essential for its activity (9). Therefore, we determined whether Y^{216} phosphorylation on GSK3β was altered after NGF deprivation by using phospho Y^{216}-specific antibodies. The phosphorylation specificity of the Y^{216} antibody was confirmed by using active rhGSK3β in the presence or absence of alkaline phosphatase (Fig. 1*C*). Furthermore, the phospho-Y^{216}-specific antibody did not detect HA-immunoprecipitated GSK3β from 293 transfected cells wherein the Y^{216} residue was mutated to phenylalanine (Y216F-GSK3β-HA, not shown). Within 1 h after NGF withdrawal, a rapid and persistent increase in GSK3β Y^{216} phosphorylation was observed, suggesting that Y^{216} phosphorylation is an early event during apoptosis (Fig. 1*D*). We also evaluated the phosphorylation of S^9, a site on GSK3β that, when phosphorylated, renders GSK3β inactive. Under basal conditions, neither S^9 nor Y^{216} phosphorylation was detected, and the low activity was confirmed by using GSK3β immunokinase assays. NGF withdrawal did not affect S^9 phosphorylation on GSK3β.

In addition to direct inhibition of GSK3β by lithium (17), insulin and lithium activate Akt and result in the subsequent inactivation of GSK3β (ref. 16 and Fig. 1*B*). Thus, we evaluated the effects on Y^{216} and S^9 phosphorylation of GSK3β by these agents. Lithium pretreatment (10 mM, 16 h) or insulin (1 μM, 3 h) addition to PC12 cells undergoing apoptosis resulted in S^9 phosphorylation (Fig. 1*E*), consistent with the notion that these agents are activating kinases that phosphorylate GSK3β on S^9. Although lithium and insulin induced S^9 phosphorylation and decreased GSK3β activity, they did not affect the NGF withdrawal-induced phosphorylation of Y^{216} (Fig. 1*F*), implying that S^9 phosphorylation is sufficient to override the Y^{216} phosphorylation-induced activation of GSK3β. This response also raises the possibility that the increased Y^{216} phosphorylation observed

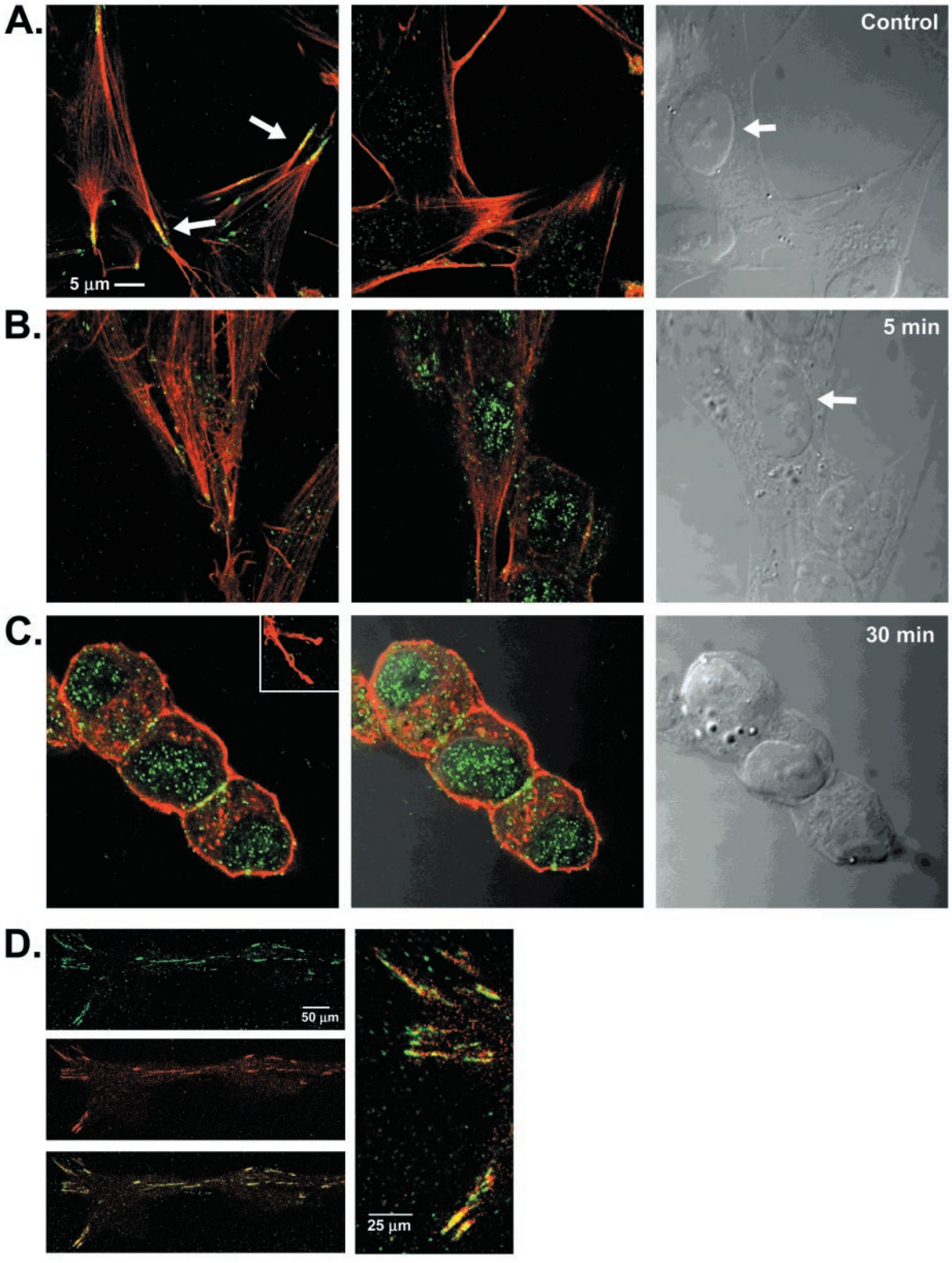

Fig. 4. Subcellular localization of phosphorylated Y^{216} GSK3β. Confocal photomicrographs: phosphorylated Y^{216} GSK3β (green), actin (red), colocalization (yellow) (*A*). (*Left*) Normal SH-SY5Y cells showing colocalization (arrow) of phosphorylated Y^{216} GSK3β and actin at focal adhesion sites. (*Center*) Minimal phosphorylated Y^{216} GSK3β (green) in the nucleus. (*Right*) Bright-field Nomarski photomicrograph of the cells showing nucleus (arrow). (*B*) Staurosporine, 5 min. (*Left*) Lack of phosphorylated Y^{216} GSK3β (green) and actin (red) colocalization at focal adhesion sites. (*Center*) Same as *Left*, at the level of the nucleus showing increase in phospho-Y^{216} immunofluorescence. (*Right*) Bright-field photomicrograph, arrow points to nucleus. (*C*) Staurosporine, 30 min. (*Left*) Lack of phosphorylated Y^{216} GSK3β (green) and actin (red) colocalization at focal adhesion sites (*Inset*) but showing increase in Y^{216} immunofluorescence at the nuclear level. (*Center*) Overlay with the Nomarski photomicrograph showing the nuclear localization of phosphorylated Y^{216} GSK3β (green). (*Right*) Bright-field Nomarski photomicrograph. (*D*) Untreated SH-SY5Y cells. Y^{216} GSK3β (green) colocalizes (yellow) with vincullin (red). (*Right*) High-power photomicrograph of the colocalized proteins.

may not be caused by autophosphorylation. To explore this possibility further, we tested whether GSK3β that completely lacks intrinsic kinase activity, i.e., K85R-GSK3β-HA could be phosphorylated at Y^{216} in response to NGF withdrawal. By using a recombinant adenovirus strategy, we achieved $\approx$90% transduction of wt GSK3β-HA and K85R-GSK3β-HA constructs (visualization of green fluorescent protein incorporated into the constructs). K85R-GSK3β-HA immunoprecipitated from cells was phosphorylated on Y^{216} similar to wt GSK3β-HA after NGF withdrawal (Fig. 1*F*). Because inactivation of GSK3β did not prevent NGF withdrawal-induced Y^{216} phosphorylation, it is likely that Y^{216} is not an autophosphorylation site.

Lithium (16 h) and insulin (3 h) also blocked NGF withdrawal-induced apoptosis (IC_{50} = 1.3 mM and 117 nM, respectively). In initial studies, the effects of lithium (10 mM) and insulin (1 μM) were examined on cell viability [by using the 3-(4,5-dimethylthiazol-2-yl)-2,5-diphenyl tetrazolium bromide (MTT) assay]. The doses of lithium and insulin used had no effect on MTT formation, indicating the lack of overt toxic effects. On treatment, cells were relatively intact and similar to NGF-differentiated PC12 cells in morphology, with extensive neurites visible (Fig. 2*A*). Because lithium is not a specific inhibitor of GSK3β, its neuroprotective effects could be mediated via other Akt-mediated survival mechanisms; therefore, we examined the effect of the K85R-GSK3β mutant on apoptosis. Compared with mock-infected PC12 cells, infection of the K85R-GSK3β mutant decreased NGF withdrawal-induced apoptosis by $\approx$60% (Fig. 2*B*). Immunokinase assays confirmed that GSK3β activity was reduced by 85% when compared with mock-infected cells, indicating that the K85R-GSK3β mutant was acting as a dominant negative protein. The cells appeared healthy with intact neurites after infection of K85R-GSK3β in NGF-deprived PC12 cells (Fig. 2*B Right*). Thus inactivation of GSK3β is critical in preventing NGF withdrawal-induced apoptosis in PC12 cells.

To evaluate whether the increase in Y^{216} phosphorylation was unique to the NGF deprivation paradigm or occurred in other models of apoptosis, we examined the responses in staurosporine-treated SH-SY5Y cells. Addition of staurosporine (100 nM) resulted in a time-dependent increase in apoptosis and in Y^{216} phosphorylation of GSK3β (Fig. 3*A*). Both lithium (IC_{50} = 13 mM) and adenoviral-mediated transduction of K85R-GSK3β blocked apoptosis induced by staurosporine, confirming the importance of GSK3β's role in neuronal apoptosis. When visualized under microscopy, >95% of the K85R-GSK3β-infected cells (multiplicity of infection = 1) showed resistance to staurosporine-induced apoptosis (see Fig. 3*B*).

To determine whether the Y^{216} phosphorylation of GSK3β was a result of autophosphorylation in the staurosporine-induced apoptosis model, we virally transduced HA-tagged wt GSK3β and K85R-GSK3β (multiplicity of infection = 100) in SH-SY5Y cells and then treated them with staurosporine. Immunoprecipitation with the anti-HA antibody and blotting with the phospho-specific Y^{216} antibody revealed that both wt GSK3β-HA and K85R-GSK3β-HA were phosphorylated at the Y^{216} site in response to staurosporine treatment (Fig. 3*C*). Because K85R-GSK3β-HA lacks intrinsic kinase activity but was Y^{216} phosphorylated on staurosporine treatment, the phosphorylation could not have occurred by autophosphorylation.

Confocal imaging was used to define the subcellular distribution of Y^{216}-phosphorylated GSK3β. In resting cells, phospho-Y^{216} immunofluorescence was observed at focal adhesion sites as defined by colocalization with the terminal regions of actin filaments (Fig. 4*A*) and the focal adhesion protein vinculin (Fig. 4*D*). Minimal Y^{216}-phosphorylated GSK3β was observed in the nucleus (Fig. 4*A Center*). In contrast, cells treated with staurosporine showed a change in the pattern of Y^{216}-phosphorylated GSK3β from focal adhesion sites to the nuclear compartment apparent as early as 5 min (Fig. 4*B*) and at 30 min after addition of 300 nM staurosporine (Fig. 4*C*). Thus the morphological changes that occur during apoptosis coincide with a differential localization of the Y^{216}-phosphorylated GSK3β. Additional experiments are necessary to determine whether this represents a translocation or simply a change in the levels of GSK3β phosphorylation within the nucleus.

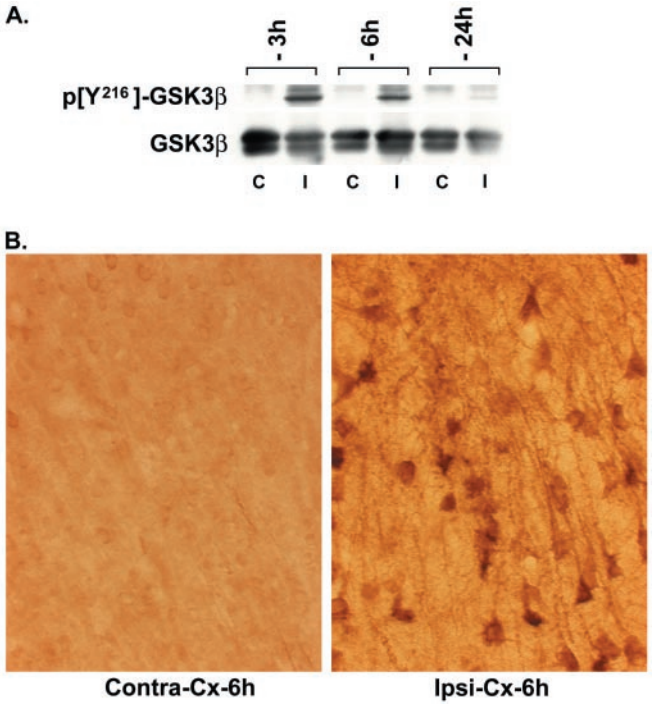

Fig. 5. Ischemia induces Y^{216} phosphorylation on GSK3β. (*A*) Western blot showing the increase in Y^{216} phosphorylation on GSK3β in the ipsilateral cortex (I) when compared with the contralateral cortex (*C*) at 3 and 6 h after MCAO. Total GSK3β in the tissue samples is shown in the lower Western blot. (*B*) Representative photomicrographs showing an increase in phosphorylated Y^{216} immunostaining in neurons in the ipsilateral (ipsi) vs. contralateral (contra) parietal cortex 6 h after MCAO.

We used focal ischemia (MCAO model) in rats to determine whether the changes observed in cell culture models were indicative of an *in vivo* response. Focal ischemia results in a loss of cortical neurons and represents an acute model of neurodegeneration. Western blot analysis revealed that as early as 3 and 6 h after MCAO, an increase in Y^{216} phosphorylation is observed in the ipsilateral but not contralateral cortex (Fig. 5*A*). Immunostaining on tissue sections showed prominent Y^{216} phosphorylation in the cortex ipsilateral to the ischemic insult (Fig. 5*B*). Preadsorption of the primary antibody with excess peptide ($\times$100) completely blocked the immunostaining (not shown). Phosphorylated Y^{216} immunostaining was localized in the cytoplasm and dendrites of the cortical pyramidal neurons; however, several neurons also exhibited nuclear immunostaining at 6 h after MCAO. Silver staining of the brains at 6 h after ischemia confirmed the presence of degenerating neurons in the cortex. S^9 phosphorylation was not altered (not shown). As demonstrated previously (15), lithium pretreatment for 16 days resulted in a significant decrease ($P < 0.05$; Student's t test) in cortical infarct volume (vehicle: 161.9 $\pm$ 15.2 mm^3; lithium: 114.1 $\pm$ 11 mm^3), raising the possibility that regulation of GSK3β activity *in vivo* may have similar effects to that described with the cell-culture models of neurodegeneration. Additional experiments are necessary to determine the regulation of the S^9 and Y^{216} phosphorylation of GSK3β by lithium in the MCAO model.

Discussion

This study provides evidence for the regulation and localization of Y^{216} phosphorylation on GSK3β in neuronal apoptosis and after ischemia in rats. The major findings are that Y^{216} phosphorylation of GSK3β occurs as part of an apoptotic response in neurons and that this site is not autophosphorylated under the conditions studied. The phosphorylation of Y^{216} was transient, preceded the induction of apoptosis, and increased in the nucleus during apoptosis. These results suggest that Y^{216} phosphorylation of GSK3β represents an important alternate mechanism by which cellular insults such as growth factor deprivation and staurosporine treatment can lead to neuronal death.

Our finding that GSK3β inhibition attenuates neuronal apoptosis is consistent with recent reports (6–8); however, the downstream mechanism is poorly understood. GSK3β phosphorylates cytosolic proteins including β-catenin and mitochondrial pyruvate dehydrogenase (18, 19), as well as nuclear proteins such as c-Jun, NFAT-c, and elongation initiation factor 2b (20, 21), yet linking the phosphorylation of any one protein to an apoptotic pathway remains controversial. GSK3β plays a key role in phosphorylating τ and promoting paired helical filament formation (11), the appearance of which is associated with early neuritic changes in Alzheimer's disease. Recently, active GSK3β localized to pretangle neurons (22). GSK3β-induced τ phosphorylation could cause neuritic dysfunction and trigger apoptosis, thereby linking two key pathologies found in Alzheimer's disease brains.

We show that Y^{216} is not subject to autophosphorylation because an inactive GSK3β mutant became Y^{216} phosphorylated in response to apoptotic stimuli. This suggests that the Y^{216} site can be phosphorylated by an upstream yet-to-be-deciphered signal transduction pathway. Recently, insulin and increased cytosolic calcium were shown to result in τ phosphorylation through an elevation of GSK3β kinase activity (23, 24). The accompanying phosphorylation on GSK3β was detected by general antiphospho-tyrosine antibodies, thus whether this represented direct phosphorylation at the Y^{216} site or an indirect inhibition of the pathway leading to S^9 phosphorylation is unclear (23). Our study provides initial evidence for the direct phosphorylation of GSK3β at the Y^{216} site by a protein kinase other than GSK3β, resulting in increased activity during apoptosis.

Under normal conditions, Y^{216}-phosphorylated GSK3β was restricted to focal adhesion sites, a localization consistent with a role for GSK3β in neurite elongation and retraction (25, 26). Several tyrosine kinases form a complex at focal adhesion sites including FAK and Fyn kinase (27, 28). Fyn coimmunoprecipitates with GSK3β in SH-SY5Y cells on insulin addition (23). In neurons, β-amyloid increases Fyn kinase and GSK3β activity (29) and inhibition of either kinase is neuroprotective (29, 30). Although it is tempting to speculate that the fyn kinase pathway results in the Y^{216} phosphorylation of GSK3β in neurons, which then translocates to the nucleus to participate in a proapoptotic cascade, further work is necessary to determine the validity of this hypothesis.

We demonstrate that after cerebral ischemia, Y^{216} phosphorylation of GSK3β is increased in neurons vulnerable to apoptosis, and lithium, a nonselective GSK3β inhibitor, was neuroprotective. Thus GSK3β could play a role in neuronal disorders in which apoptosis has been suggested as a common molecular mechanism. If this is true, GSK3β inhibitors would be therapeutically useful in attenuating the course of both acute and chronic neurodegenerative diseases.

We thank Richard Lampe, Youjun Chen, My Linh Do, Linda Foster-Brown, and Rebecca Kozel for technical assistance, Dr. Timothy Piser for suggestions, and Drs. Alan Cross, Ladislav Mrzljak, and Michael Klimas for support.

1. Raff, M. C., Barres, B. A., Burne, J., Coles, H. S., Ishizaki, Y. & Jacobson, M. D. (1993) *Science* **262,** 695–700.
2. Stefanis, L. Burke, R. E. & Greene, L. A. (1997) *Curr. Opin. Neurol.* **10,** 299–305.
3. Yao, R. & Cooper G. M. (1995) *Science* **267,** 2003–2006.
4. Dudek H., Datta, S. R., Franke, T. F., Birnbaum, M. J., Yao, R. J. Cooper, G. M., Segal, R. A., Kaplan, D. R. & Greenberg, M. E. (1997) *Science* **275,** 661–665.
5. Franke, T. F., Kaplan, D. R. & Cantley, L. C. (1997) *Cell* **88,** 435–437.
6. Pap, M. & Cooper, G. M. (1998) *J. Biol. Chem.* **273,** 19929–19932.
7. Hetman, M., Cavanaugh, J. E., Kimelman, D. & Xia, Z. (2000) *J. Neurosci.* **20,** 2567–2574.
8. Bijur, G. N., De Sarno, P. & Jope, R. S. (2000) *J. Biol. Chem.* **275,** 7583–7590.
9. Hughes, K., Nikolakaki, E., Plyte, S. E., Totty, N. F. & Woodgett, J. A. (1993) *EMBO J.* **12,** 803–808.
10. Shaw, M., Cohen, P. & Alessi, D. A. (1997) *FEBS Lett.* **416,** 307–311.
11. Lovestone, S., Reynolds, C. H., Latimer, D., Davis, D. R., Anderton, B. H., Gallo, J.-M., Hanger, D., Mulot, S., Marquardt, B., Stabel, S., *et al*. (1994) *Curr. Biol.* **4,** 1077–1086.
12. Wagner, U., Utton, M., Gallo, J. M. & Miller, C. C. (1996) *J. Cell Sci.* **109,** 1537–1543.
13. Sutherland, C., Leighton, I. A. & Cohen, P. (1993) *Biochem. J.* **296,** 15–19.
14. Bhat, R. V., Engber, T., Finn, J. P., Koury, E. J., Contreras, P. C., Miller, M., Dionne, C. A. & Walton, K. M. (1998) *J. Neurochem.* **70,** 558–571.
15. Nonaka, S. & Chuang, D. M. (1998) *NeuroReport* **9,** 2081–2084.
16. Chalecka-Franaszek, E. & Chuang, D. M. (1999) *Proc. Natl. Acad. Sci. USA* **96,** 8745–8750.
17. Klein, P. S. & Melton, D. A. (1996) *Proc. Natl. Acad. Sci. USA* **93,** 8455–8459.
18. Ikeda, S., Kishida, S., Yamamoto H, Murai, H., Koyama, S. & Kikuchi, A. (1998) *EMBO J.* **17,** 1371–1384.
19. Hoshi, M., Takashima, A., Noguchi, K., Murayama, M., Sato, M., Kondo, S., Saitoh, Y., Ishiguro, K., Hoshino, T. & Imahori, K. (1996) *Proc. Natl. Acad. Sci. USA* **93,** 2719–2723.
20. Graef, I. A., Mermelstein, P. G., Stankunas, K., Neilson, J. R., Deisseroth, K., Tsien, R. W. & Crabtree, G. R. (1999) *Nature (London)* **401,** 703–708.
21. Woodgett, J. R., (1990) *EMBO J.* **9,** 2431–2438.
22. Pei, J. J., Braak, E., Braak, H., Grunde-Iqbal, I., Iqbal, K., Winblad, B. & Cowburn, R. F. (1999) *J. Neuropath. Exp. Neurol.* **58,** 1010–1019.
23. Lesort, M., Jope, R. S. & Johnson, G. V. (1999) *J. Biol. Chem.* **72,** 576–584.
24. Hartigan, J. A. & Johnson, G. V. (1999) *J. Biol. Chem.* **274,** 21395–21401.
25. Sayas, C. L., Moreno-Flores, M. T., Avila, J. & Wandosell, F. (1999) *J. Biol. Chem.* **274,** 37046–37052.
26. Takahashi, M., Yasutake, K. & Tomizawa, K. (1999) *J. Neurochem.* **73,** 2073–2083.
27. Lauri, S. E., Taira, T. & Rauvala, H. (2000) *NeuroReport* **11,** 997–1000.
28. Chen, L. M., Bailey, D. & Fernandez-Valle, C. (2000) *J. Neurosci.* **20,** 3776–3784.
29. Takashima, A., Honda, T., Yasutake, K., Michel, G., Murayama, O., Murayama, I., Ishiguro, K. & Yamaguchi, H. (1998) *Neurosci. Res.* **31,** 317–323.
30. Lambert, M. P., Barlow, A. K., Chromy, B. A., Edwards, C., Freed, R., Liosatos, M., Morgan, T. E., Rozovsky, I., Trommer, B., Viola, K. L., *et al*., (1998) *Proc. Natl. Acad. Sci. USA* **95,** 6448–6453.